

Electronic Supplementary Information for

A new automated synthesis of a coke-resistant Cs-promoted Ni-supported nanocatalyst for sustainable dry reforming of methane

Kyung Hee Oh^{a,c}, Jin Hee Lee^a, Kwangsoo Kim^b, Hack-Keun Lee^a, Shin Wook Kang^a, Jung-Il Yang^a, Jong-Ho Park^a, Chang Seop Hong^{c,}, Byung-Hyun Kim^{b,*}, and Ji Chan Park^{a,d,*}*

^a Clean Fuel Laboratory, Korea Institute of Energy Research, Daejeon, 34129, Korea.

^b Computational Science & Engineering Laboratory, Korea Institute of Energy Research, Daejeon, 34129, Korea.

^c Department of Chemistry, Korea University, Seoul, 02841, Korea.

^d Advanced Energy and System Engineering, University of Science and Technology, Daejeon, 34113, Korea.

E-mail: cshong@korea.re.kr (C. S. Hong), bhkim@kier.re.kr (B.-H. Kim), and jcspark@kier.re.kr (J. C. Park)

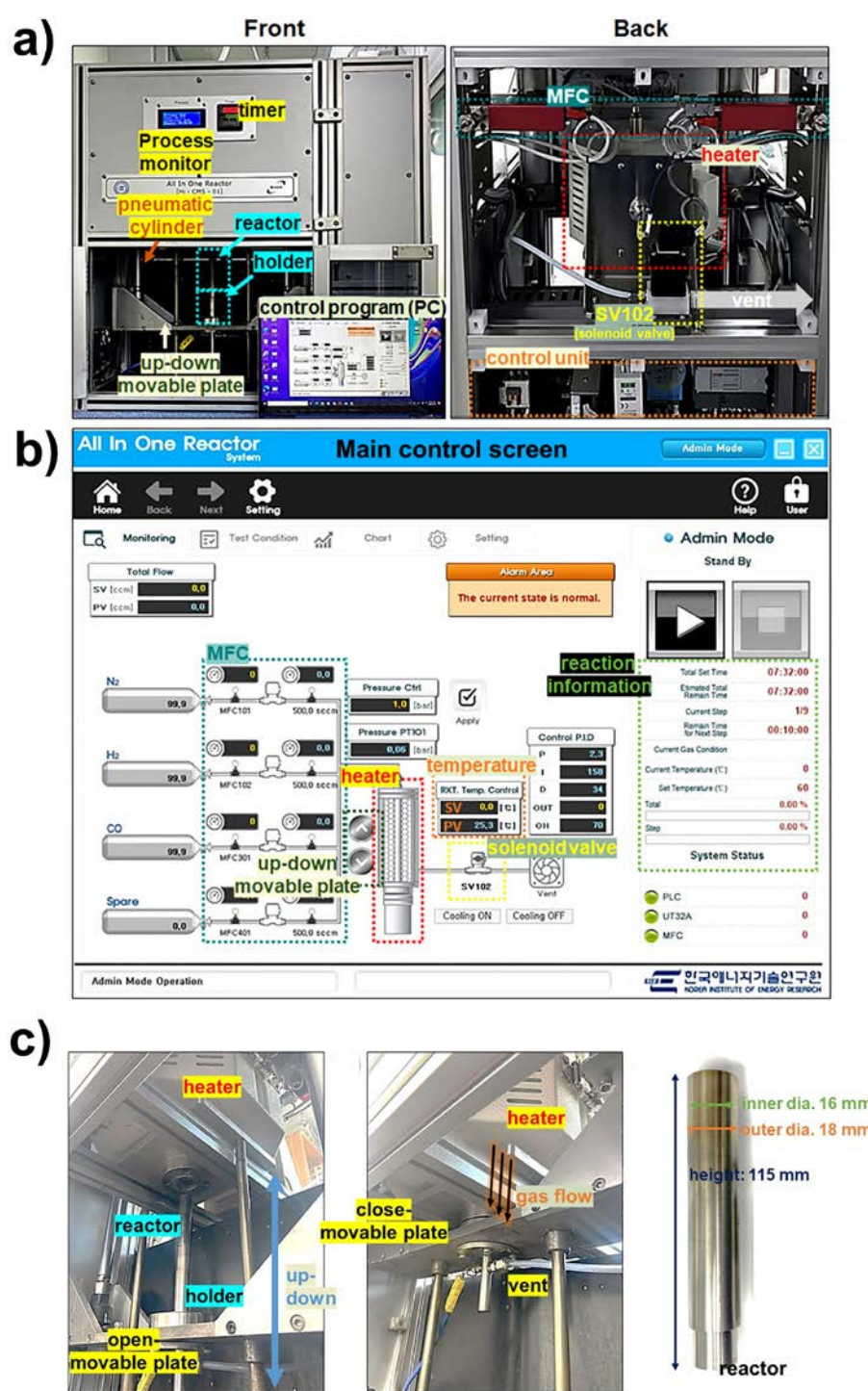


Figure S1. (a) Photographs of the AIO apparatus, (b) control program, and (c) the reactor and the loading system by a movable plate with a stainless steel reactor used for catalyst synthesis.

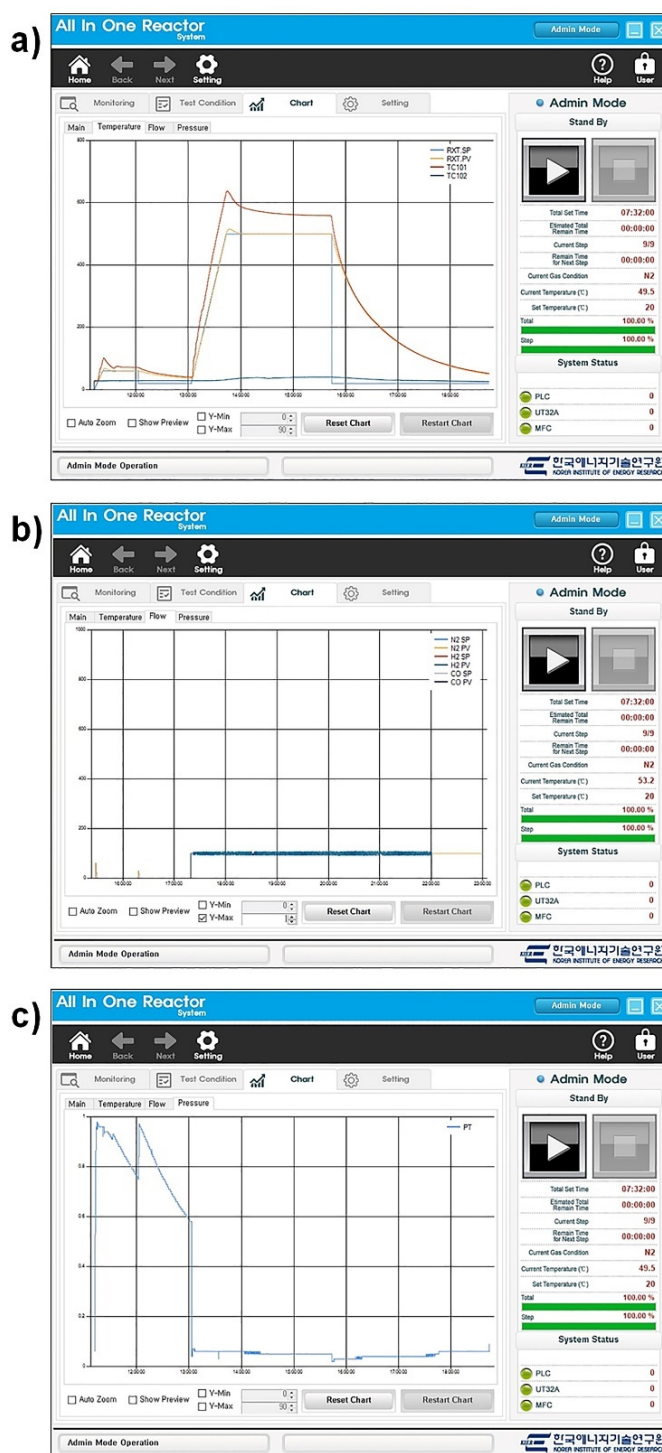


Figure S2. Screenshots in the control program for the real-time data (a: temperature, b: gas flow, c: pressure).

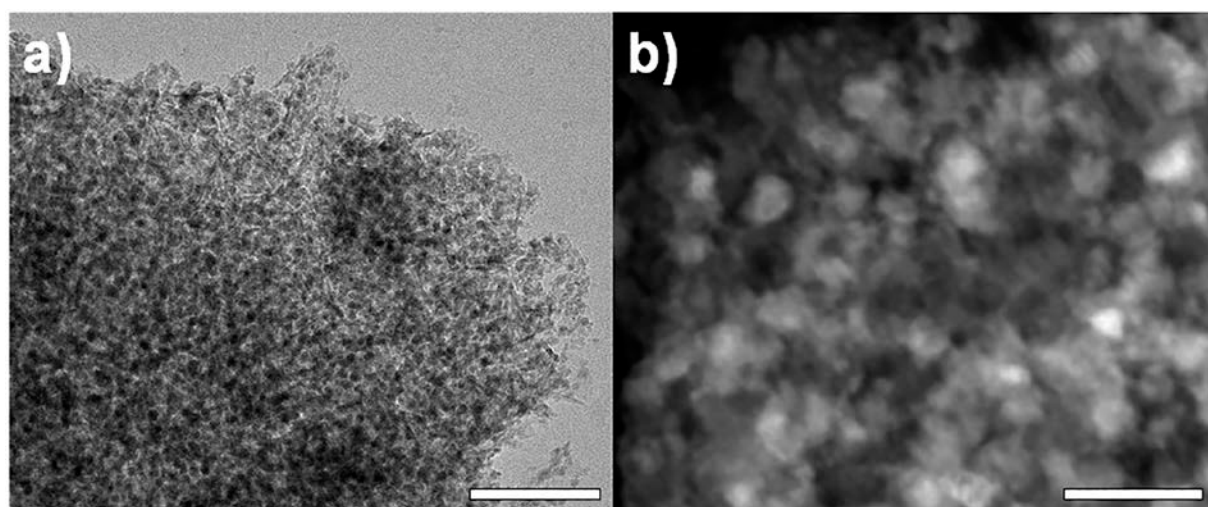


Figure S3. (a) Low-resolution TEM and (b) HAADF-STEM images of the U-(Cs)Ni/Al₂O₃ nanocatalyst. The bars represent 100 nm (a) and 20 nm (b).

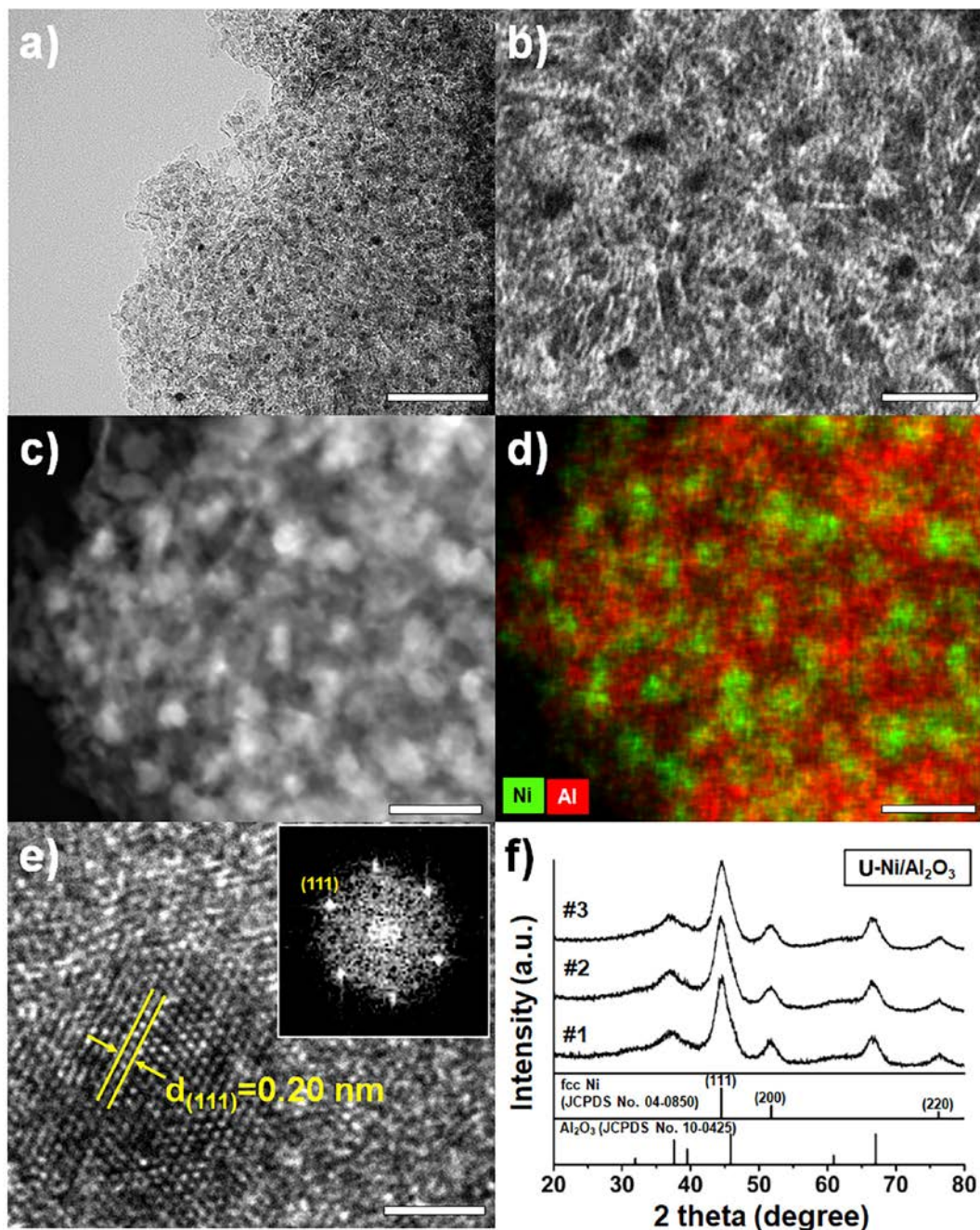


Figure S4. (a) Low-resolution and (b) magnified TEM images, (c) HAADF-STEM image, (d) elemental mapping image, and (e) HR-TEM image with corresponding FT pattern (inset of e) of U-Ni/Al₂O₃ nanocatalyst. (f) XRD spectra of the U-Ni/Al₂O₃ nanocatalysts in three different batches. The bars represent 100 nm (a), 20 nm (b-d), and 2 nm (e).

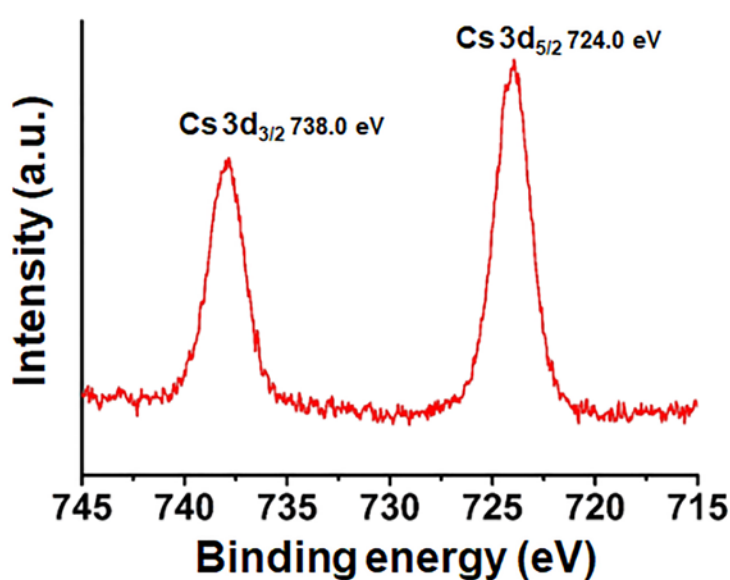


Figure S5. XPS spectrum in the energy region of the Cs 3d in U-(Cs)Ni/Al₂O₃ nanocatalyst.

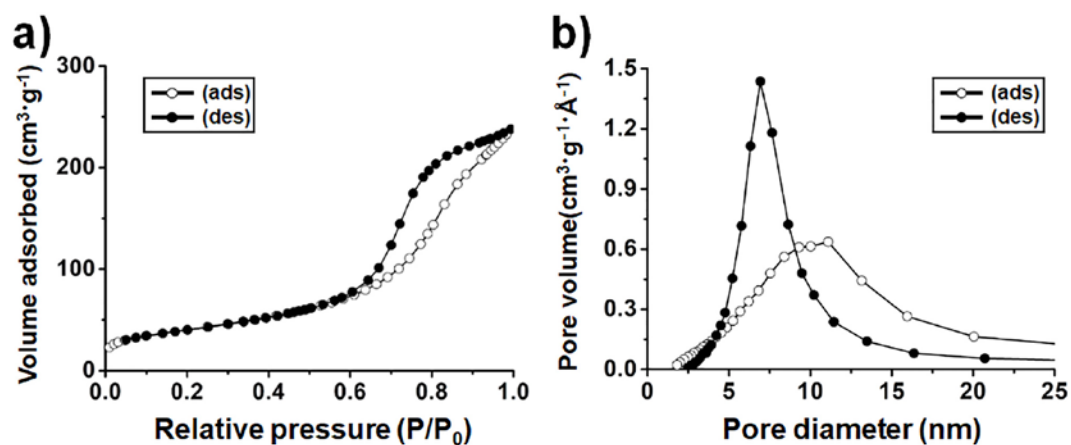


Figure S6. (a) N₂ sorption isotherms and (b) Pore size distribution diagram of the U-Ni/Al₂O₃ nanocatalyst.

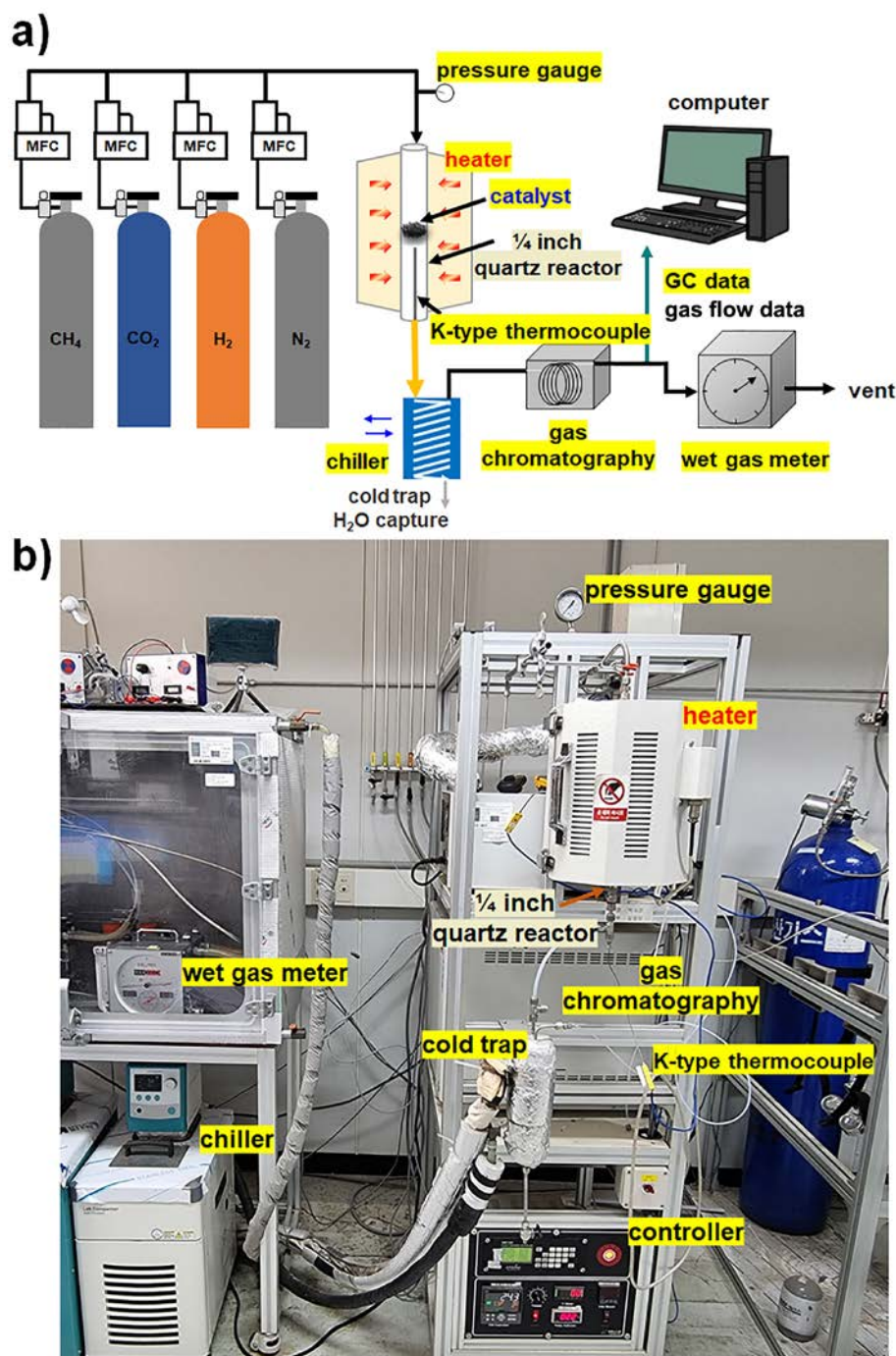


Figure S7. (a) Schematic diagram and (b) Picture of the DRM reaction system.

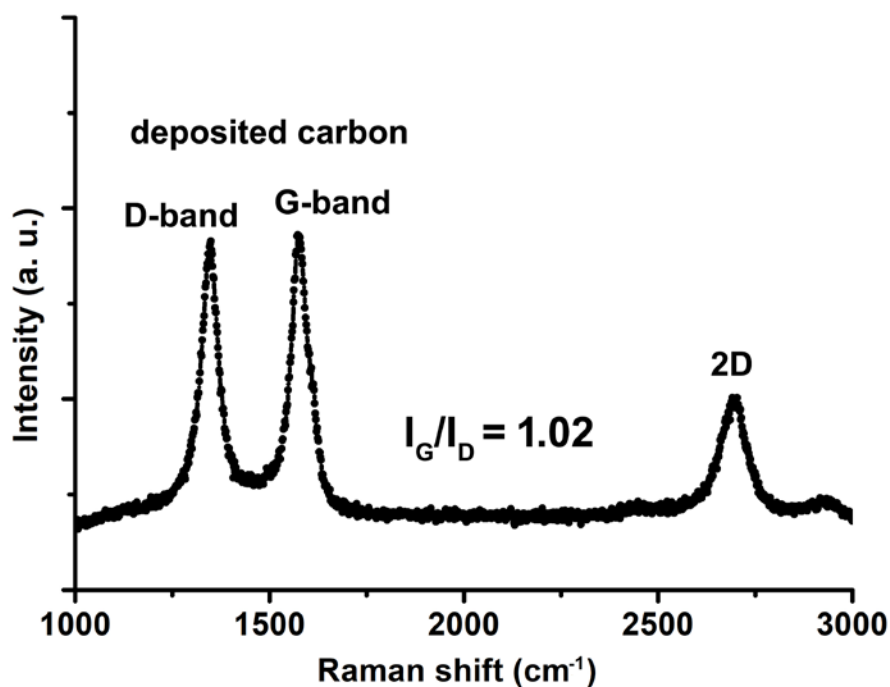


Figure S8. Raman spectrum of Cs-free U-Ni/Al₂O₃ nanocatalyst recovered after the DRM reaction under GHSV=72 NL·g_{cat}⁻¹·h⁻¹ at 800 °C.

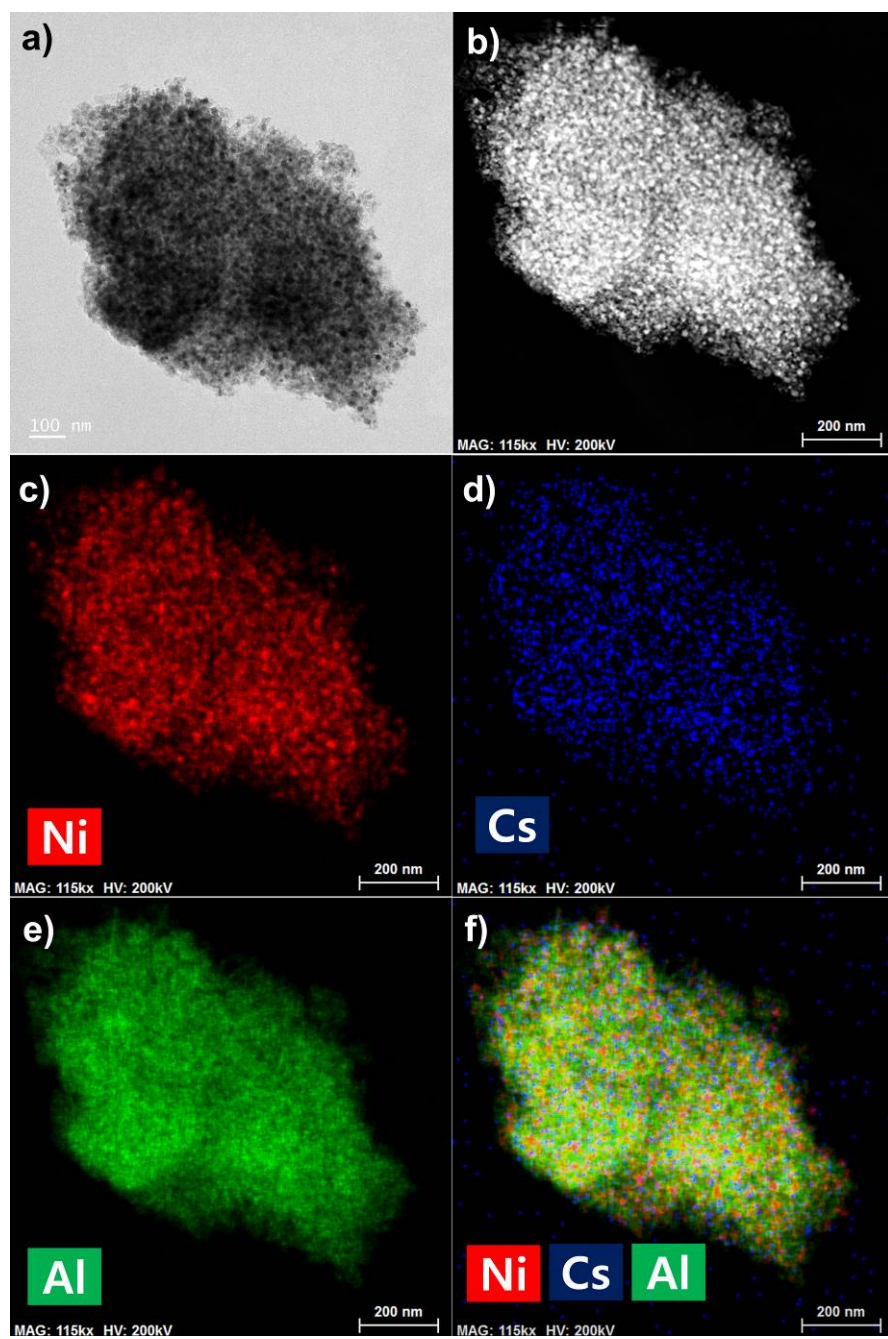


Figure S9. (a) TEM image, (b) HAADF-STEM image, and (c-f) elemental mapping images of the spent U-(Cs)Ni/Al₂O₃ nanocatalyst recovered after the DRM reaction under GHSV=72 NL·g_{cat}⁻¹·h⁻¹ at 800 °C.

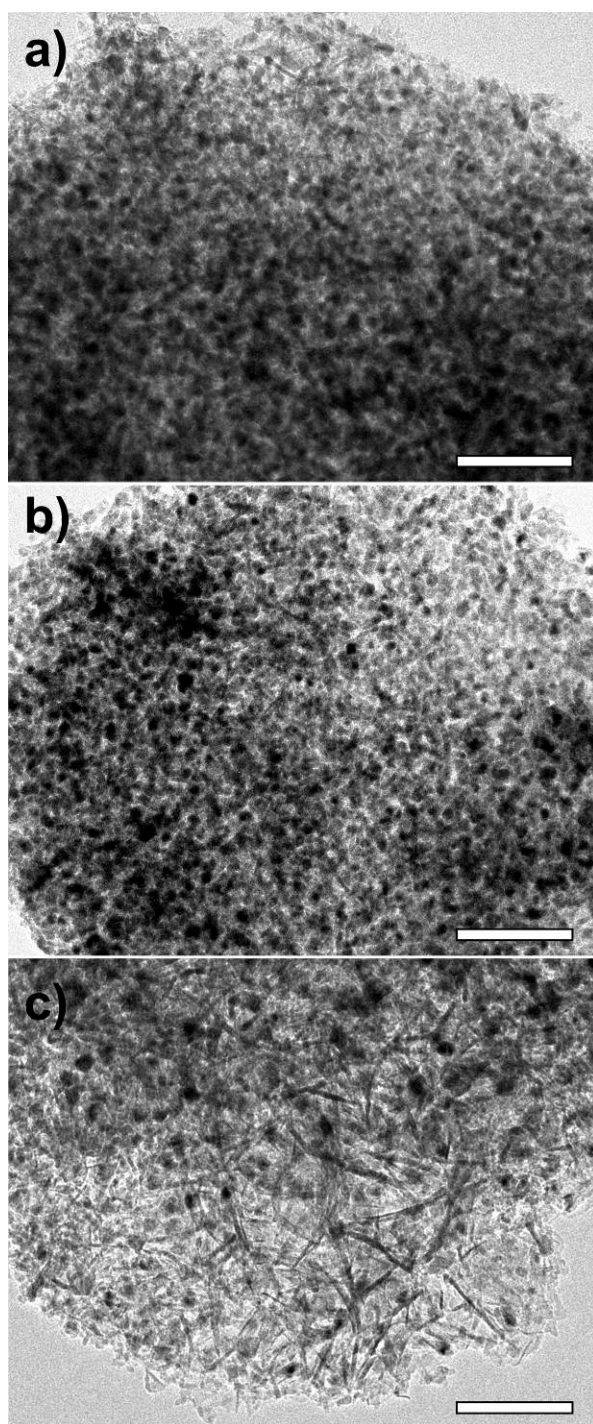


Figure S10. Low-resolution TEM images of (a) fresh U-(Cs)Ni/Al₂O₃ nanocatalyst, (b) U-(Cs)Ni/Al₂O₃ after thermal treatment under a H₂ flow at the reaction temperature (800 °C), and (c) recovered U-(Cs)Ni/Al₂O₃ after the DRM reaction under GHSV=72 NL·g_{cat}⁻¹·h⁻¹ at 800 °C. All bars represent 100 nm.

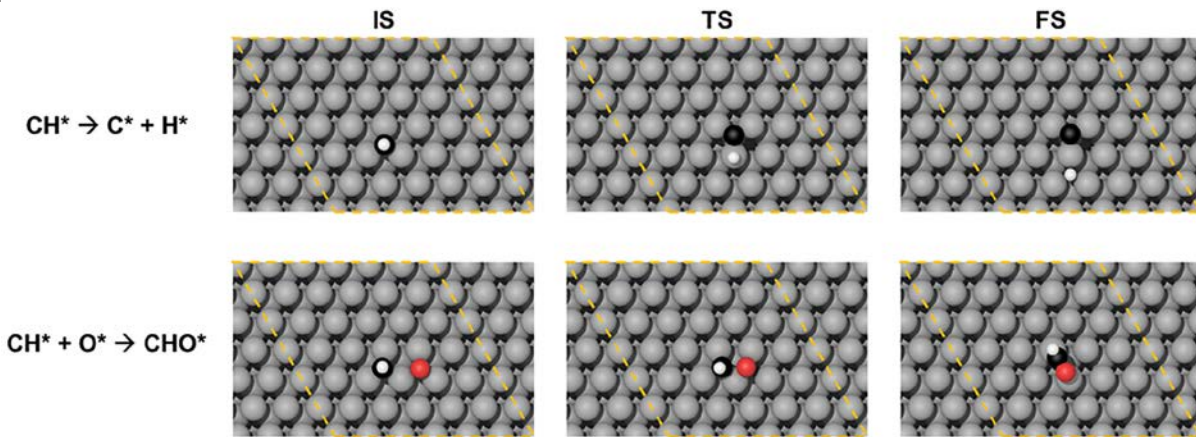


Figure S11. Geometry optimized structures of the CH^* dehydrogenation and oxidation steps for the bare Ni (111) surface. Grey, black, red, and white balls represent Ni, C, O, and H atoms, respectively. Yellow dashed lines in the atomic structures indicate the supercell used in this work.

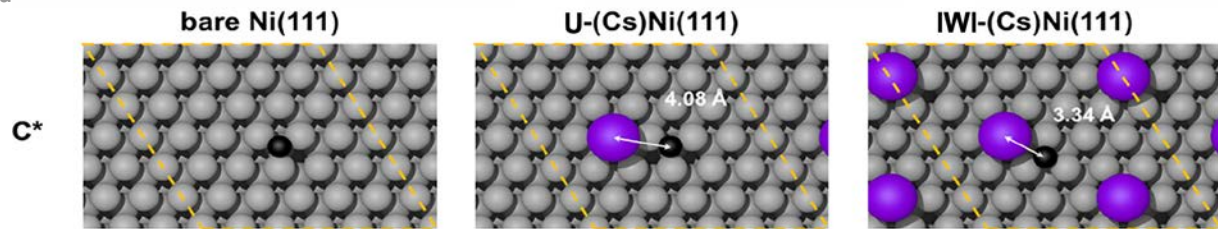


Figure S12. Geometry optimized structures for the most stable adsorption site of C on bare Ni (111), U-(Cs)Ni (111), and IWI-(Cs)Ni (111).

Table S1. An optimized sequence data for the synthesis of U-(Cs)Ni/Al₂O₃ nanocatalysts.^{a)}

Step conditions	1	2	3	4	5	6	7	8	9
Set Reaction Temp. (°C)	60	60	20	20	500	500	20	20	20
Time (min)	10	40	1	60	40	120	1	120	60
N ₂ flow (mL·min ⁻¹)	0	0	0	0	0	0	0	0	100
H ₂ flow (mL·min ⁻¹)	0	0	0	0	100	100	100	100	0
Stage	Aging			Heating	Calcination		Cooling		Purge

^{a)} The trend data with real-time monitoring during the whole synthesis procedure are shown in the attached movie S1.

Table S2. Comparison of Ni-based catalysts for dry reforming of methane at a reaction temperature of 800 °C.

Catalyst	GHSV (NL·g _{cat} ⁻¹ ·h ⁻¹)	CH ₄ /CO ₂ /inert gas	CH ₄ Conv. (%) ^{a)}	CO ₂ Conv. (%) ^{a)}	carbon deposition rate (mg _{carbon} ·g _{cat} ⁻¹ ·h ⁻¹)	ref.
U-(Cs)Ni/Al ₂ O ₃		1/1	89.8	91.8	4.7 (1.87 wt % loss in TGA)	
U-Ni/Al ₂ O ₃	72	1/1	86.9	88.5	30 (12.0 wt % loss in TGA)	This work
commercial Ni cat.		1/1	67.3	77.6	78.1 (31.2 wt % loss in TGA)	
Ni@Al ₂ O ₃ (Ni: 12 wt%)	36	1/1	86	82	3.0 (15.0 wt % loss in TGA)	[1]
Ni-Ca-4	14.4	1:1	52	96.7	42.9 (18.0 wt% loss in TGA)	[2]
La-Ni-1 (Ni: 9.6 wt%)	14.4	1:1	94.3	96.6	7.0 (5.6 wt% loss in TGA)	[3]
Ni@SiO ₂ (Ni: 18.6 wt%)	36	1/1/1	90	95	No carbon in TGA	[4]
Ni/Al ₂ O ₃ nanosheet-uncal (Ni: 10wt%)	108	1/1.05/1	92	95	280 (35 wt % loss in TGA)	[5]
0.5Ni/CeNi _x O _y (Ni: 15.1 wt%)	36	1/1/1	86.2	87.7	45 (47.1 wt% loss in TGA)	[6]
Ni@SiO ₂ /Al ₂ O ₃ /FeCrAl- fiber (Ni: 32.68 wt%)	5	1/1.1	90.8	89.9	No carbon in TGA	[7]
Ni/Al ₂ O ₃ -Y ₂ O ₃ -3%Nd ₂ O ₃ (Ni: 10.22wt%)	27	1/1/0.6	88.5	92.2	10.8 (6.47 wt% loss in TGA)	[8]

^{a)} The conversion rates are obtained from the final data point of each reaction.

References)

- [1] Q. Huang, X. Fang, Q. Cheng, Q. Li, X. Xu, L. Xu, W. Liu, Z. Gao, W. Zhou and X. Wang, *ChemCatChem*, 2017, **9**, 3563.
- [2] H. Wang, W. Mo, X. He, X. Fan, F. Ma, S. Liu and D. Tax, *ACS Omega*, 2020, **5**, 28955.
- [3] W. Mo, F. Ma, Y. Ma and X. Fan, *Int. J. Hydrogen Energy*, 2019, **44**, 24510.
- [4] Z. Li, L. Mo, Y. Kathiraser and S. Kawi, *ACS Catal.*, 2014, **4**, 1526.
- [5] W. Y. Kim, Y. H. Lee, H. Park, Y. H. Choi, M. H. Lee and J. S. Lee, *Catal. Sci. Technol.*, 2016, **6**, 2060.
- [6] J. Dou, Z. Bao and F. Yu, *ChemCatChem*, 2018, **10**, 250.
- [7] R. Chai, G. Zhao, Z. Zhang, P. Chen, Y. Liu and Y. Lu, *Catal. Sci. Technol.*, 2017, **7**, 5500–5504
- [8] R. Zhu, X. Ding, Z.R. Liu, Y.A. Li, L. Wu, L. Zheng and Y. Wang, *Catal. Lett.*, 2022, doi.org/10.1007/s10562-022-03956-x.

Table S3. Calculated adsorption energy of each adsorbate and its corresponding most stable adsorption site during the DRM process for bare Ni (111), U-(Cs)Ni (111), and IWI-(Cs)Ni (111).

Adsorbate	Adsorption energy (eV) / Adsorption site		
	bare Ni (111)	U-(Cs)Ni (111)	IWI-(Cs)Ni (111)
CH ₃	-2.28 / fcc hollow	-2.21 / fcc hollow	-2.14 / fcc hollow
CH ₂	-4.31 / fcc hollow	-4.37 / fcc hollow	-4.34 / fcc hollow
CH	-6.74 / fcc hollow	-6.83 / fcc hollow	-6.81 / fcc hollow
C	-7.11 / hcp hollow	-7.18 / hcp hollow	-7.31 / fcc hollow
CHO	-2.38 / bridge	-2.47 / hcp hollow	-2.45 / atop
CO	-2.13 / hcp	-2.28 / hcp hollow	-2.47 / fcc hollow
CO ₂	-0.01 / bridge	-0.38 / bridge	-0.81 / bridge
O	-5.60 / fcc hollow	-6.03 / fcc hollow	-6.06 / fcc hollow
H	-2.95 / fcc hollow	-3.00 / fcc hollow	-3.01 / fcc hollow

Captions for Movie

Movie S1. In situ synthesis monitoring by the automated AIO reaction system from start to end.